Available online at http://scik.org

Commun. Math. Biol. Neurosci. 2023, 2023:121

https://doi.org/10.28919/cmbn/7931

ISSN: 2052-2541

THE EFFECT OF STRUCTURAL REINFORCEMENT IN THE SOLID ANKLE FOOT ORTHOSIS: A FINITE ELEMENT ANALYSIS

ALFIAN PRAMUDITA PUTRA[1,2,*], MOHAMMAD RIZKI DWIATMA[1], AKIF RAHMATILLAH[1,2], PUJIYANTO[3], DWI MELLY APRILIA SARI[1], OSMALINA NUR RAHMA[1,2], DITA AYU MAYASARI[4], I PUTU ALIT PAWANA[5]

[1]1Biomedical Engineering, Department of Physics, Faculty of Science and Technology, Universitas Airlangga, Surabaya, 60115, Indonesia

[2]Biomedical Signals and Systems Research Group, Faculty of Science and Technology, Universitas Airlangga, Surabaya, 60115, Indonesia

[3]Department of Physics, Faculty of Science and Technology, Universitas Airlangga, Surabaya, Indonesia, Surabaya, 60115, Indonesia

[4]Biomedical Engineering Study Program, Faculty of Engineering, Universitas Dian Nuswantoro, Semarang, 50131, Indonesia

[5]Department of Rehabilitation and Physical Medicine, Dr. Soetomo General Academic Hospital, Surabaya, 60248, Indonesia

Abstract: Background: Solid Ankle Foot Orthosis (SAFO) has the ability to hold the plantarflexion and dorsiflexion. It helps improve foot clearance which can stop foot drop. During gait, it usually possesses a specific area with high pressure due to gait that leads to cracks in that particular area. Structural reinforcement can be introduced to tackle this problem. This study aims to observe the effect of structural reinforcements on SAFO's stiffness against the force generated during the stance phase and to find out which parameter combination gives the best results.

Methods: The SAFO was designed into 3 models, SAFO variation I without reinforcement, SAFO variation II with reinforcement of 260 mm, and SAFO variation III with reinforcement of 130 mm. Carbon fiber (CF) and

*Corresponding author

E-mail address: alfian.pramudita@fst.unair.ac.id

Received February 28, 2023

polypropylene (PP) were used as materials in the simulation. The SAFO models were analyzed by the Finite Element Method in the gait cycle and cuff loading simulation.

Results: The simulation showed that the SAFO toughness and stiffness increased as the increase in length of the reinforcement was applied. CF material provided better toughness and stiffness than PP. CF AFO variation II had the highest toughness during the gait cycle simulation. During cuff loading simulation, CF AFO variation II had the highest level of stiffness with a rotational stiffness ratio of 246.52 Nm/°.

Conclusions: The presence of structural reinforcement in SAFO affects the toughness and stiffness of SAFO.

Keywords: solid ankle foot orthosis; foot drop; post-stroke; rehabilitation; reinforcement; healthcare.

2020 AMS Subject Classification: 92C50.

1. INTRODUCTION

Stroke is one of the leading causes of disability worldwide [1]. The abnormality of gait includes a wide range of total patients who have recovered from the stroke. Around 20-30% of the patients who survived the acute stroke lost their ability to walk, and some needed an assistive device to do their daily activities [2]. Post-stroke gait is characterized by reduced walking speed, increased energy consumption, asymmetry, drop foot, and lack of muscle activity in the stance phase of the gait cycle [3].

A drop foot is a symptom of a neuromuscular disorder that can be temporary or permanent. In patients with drop foot, the tibialis anterior muscle experiences weakness, eliminating the patient's ability to perform dorsiflexion to lift the forefoot from the ground [4]. 20% of post-stroke patients have suffered from foot drops [5].

Apart from drop foot abnormalities, post-stroke gait is also characterized by less muscle activity during the stance phase. A heel rise indicates the transition from the mid-stance to the terminal stance. The heel rise begins with the internal plantarflexion motion of the ankle, and later the foot will do a pushing force on the ground to make a progressive push forward for propulsion. Under normal conditions, the calf muscles will reach a peak of contraction during the terminal stance. This contraction compensates for the emergence of an external moment from the push of the foot against the ground during heel rise [6].

AFO is commonly divided into two types which are passive and active AFO, which has a control system that can adapt to the human gait [7]. Moreover, the passive AFO is divided into two types which are articulated and non-articulated AFO, which could be used by post-stroke patients with insufficient balance and unstable stature [8].

Solid-type AFOs (SAFO) can be applied to post-stroke patients with weakness of the tibialis anterior muscles (dorsiflexion muscles) and calf muscles that function as compensators for heel rises. This condition can be achieved because SAFO prevents plantarflexion and dorsiflexion [9]. When plantarflexion is restricted, the drop foot problem is resolved and provides better foot clearance. In addition, restriction of plantarflexion will inhibit the heel-rise process and eliminate the terminal stance phase. In this condition, the function of the calf muscles weakened in post-stroke patients in stabilizing the gait process is no longer needed [10].

Most of the AFOs are custom-fabricated, accounting for 73%. On the other hand, the most frequently used material is thermoplastic, with a percentage of 83%. This production process takes a long time and is done manually, where the skills of the orthotics matter and will determine the quality of the fabricated AFO. Therefore, the existence of an initial quantification to measure the character of AFO, which is a crucial factor such as stiffness and thickness, will be very beneficial in determining the extent of resistance that can be given by an AFO [11].

Orthosis fabrication processes such as AFO can be carried out using Computer-Aided Design (CAD) and Computer-Aided Manufacture (CAM) to improve the quality of health services for rehabilitation patients [12-14]. The application of both can be reflected in using the Finite Element Method (FEM) in modeling AFO in a specific patient. This method allows orthotics to measure the mechanical behavior and distribution of stress concentrations before the AFO manufacturing process. The existence of this process will reduce the occurrence of errors so that it will save time and wasted fabrication material [11].

SAFO will experience mechanical compressive forces during the gait cycle, leading to a critical point where it will eventually lead to cracks in several specific areas of the SAFO. Orthotics solved this problem by applying structural reinforcements of various particular shapes and different positioning positions. As a result, prefabricated SAFO has a fracture ratio of one to two

relative to custom SAFOs [15]. In their research, Gomes et al. [16] used structural reinforcements on retromalleolar sections with different dimensions. As a result, the thickest reinforcement provides the best endurance.

2. METHODS

The design phase of the SAFO 3D model was carried out using Autodesk Fusion 360. Fig. 1 shows the 3D SAFO model designed to vary in the length of reinforcements. Variations in the reinforcement length applied to the models are 260 mm, 130 mm, and without reinforcement. The thickness of the reinforcements was 6 mm in all models.

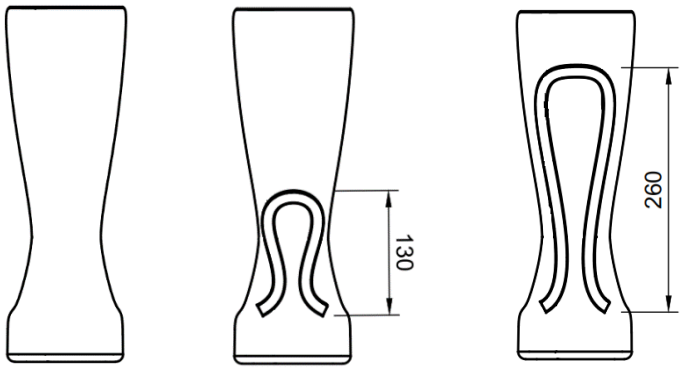

(a) (b) (c)

Fig. 1. The dimension of reinforcements for each SAFO variation. (a) Model I, (b) Model II, (c) Model III (Unit in mm)

The simulation started with selecting the material that forms the SAFO model. The materials used are carbon fiber (CF) and polypropylene (PP). After choosing the material, the boundary conditions were set, including fixed support and the direction and magnitude of the applied load. The load was applied to the hindfoot, midfoot, and forefoot. These loads represent human gait at initial contact, midstance, and terminal stance. The magnitude of the applied loads was 500 N. Apart from describing the external force during the gait cycle, the loading was also applied to the posterosuperior part of the SAFO. The loading was directed perpendicular to the sagittal plane,

pointing towards the medial region of the SAFO. This loading was used to measure the stiffness of the SAFO models.

A convergence study was conducted to find the optimal mesh size for the entire simulation [17, 18]. The model design used as an experimental model during the convergence study was model III (reinforcement length of 260 mm). The simulation carried out as the convergence study is the initial contact during the gait cycle. Convergence study results are shown in Fig. 2.

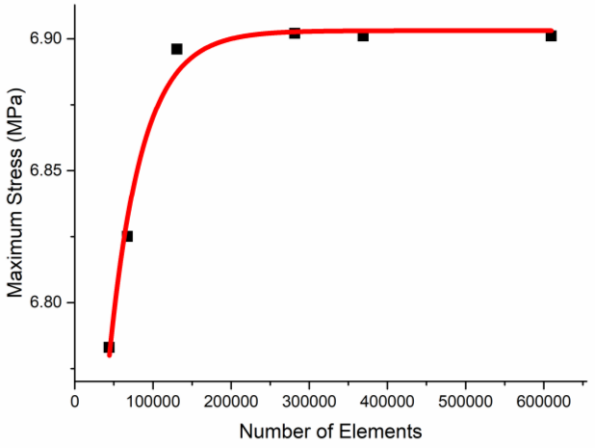

Fig. 2. Convergence Study of SAFO Model

Fig. 2 showed that the stress simulation results were stable or convergent from the number of elements 130917 to 609675. Therefore, the number of features 281375 was considered an optimal choice. The results of this convergence study indicated that a mesh size of 0.003 m was the optimal size. This mesh size was used throughout the simulation. The convergence study process with the same method has also been carried out by Basri et al. [19].

The model's mechanical behavior in response to loading was analyzed. The stress simulation results were used in Equation 1 to calculate the value of the safety factor. The safety factor is calculated by dividing the maximum stress the material can withstand by the equivalent pressure obtained from the simulation [20]. The safety factor shows the safety level of the simulated model. A high safety factor value indicates that the AFO has high endurance [21]. Therefore, it can be said that the AFO model is safe to use.

$$Safety\ Factor = \frac{Ultimate\ Tensile\ Strength}{Maximum\ Stress} x100\% \quad (1)$$

The level of stiffness of each model analysis was also carried out. It was determined from the deformation result of posterosuperior AFO (cuff area) loading simulation. Fig. 3 shows the schematic calculation of the level of stiffness of the AFO.

The highest deformation value in the simulation was used in Eq. 2 to obtain the angular deflection. The angular deflection results from Eq. 2 were utilized in Eq. 3 to determine the ratio of rational stiffness, whose value will represent the AFO models stiffness level. Analysis of the level of stiffness using rational stiffness has also been carried out previously by Chen et al. [15].

$$\theta = tan^{-1}(\frac{x}{r}) \quad (2)$$

$$Rotational\ Stiffness = \frac{F.r}{\theta} \quad (3)$$

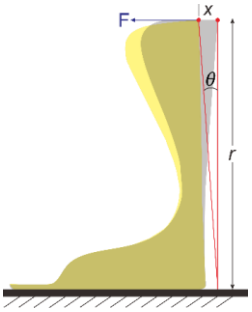

Fig. 3. SAFO Stiffness Level Calculation. Note: (x) Highest Deformation in Cuff Loading Simulation, (r) AFO Height, (F) Applied Force, (θ) Angle Deflection

3. RESULTS

Gait cycle loading was carried out to analyze the resistance of AFO during use. In this simulation, a static force of 500 N is used, which represents the vertical component of the Ground Reaction Force (GRF) that arises during the gait cycle. The stress distribution during GRF loading was shown in Figures 4 and 5 for three different models and two materials.

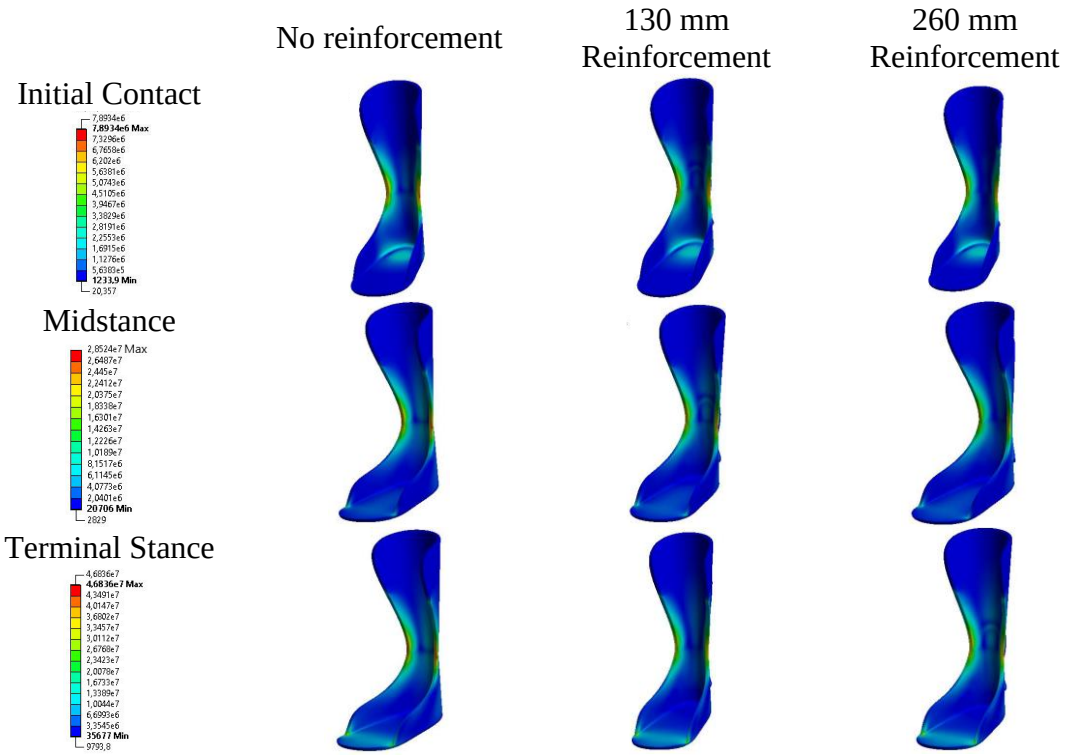

Fig. 4. Stress Distribution of Three PP SAFO Models with Different Structural Reinforcement in Three Subphases (Initial Contact, Midstance, and Terminal Stance)

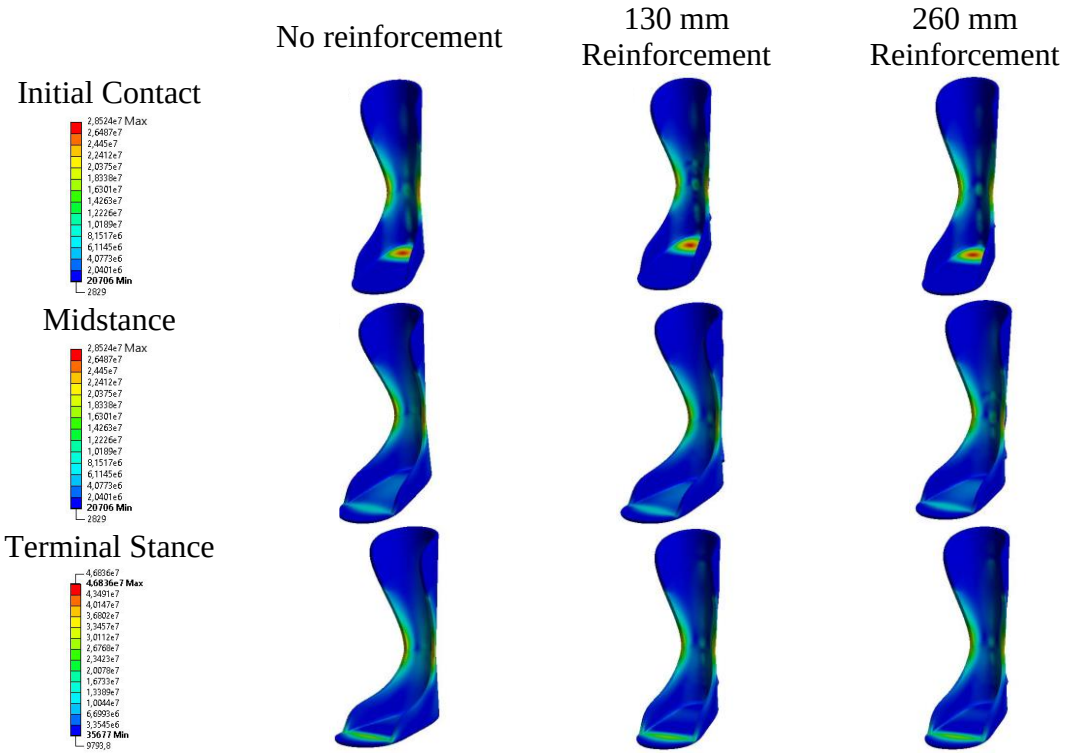

Fig. 5. Stress Distribution of Three CF SAFO Models with Different Structural Reinforcement in Three Subphases (Initial Contact, Midstance, and Terminal Stance)

The von Mises stress data were used to calculate the safety factor of the model. The safety factor of the model is depicted in Figure 6. SAFO with CF material had a higher safety factor than with PP material. The material's Ultimate Tensile Strength (UTS) had a significant role in obtaining safety factors. Regarding subphases, the safety factor is the highest during initial contact. This condition indicated that both SAFO was safe during the initial contact. The concern from the result in Figure 6 was on the midstance and terminal stance for SAFO with PP material, which showed a value under 100%. This result indicated that the SAFO would be prone to crack or failure during those two subphases.

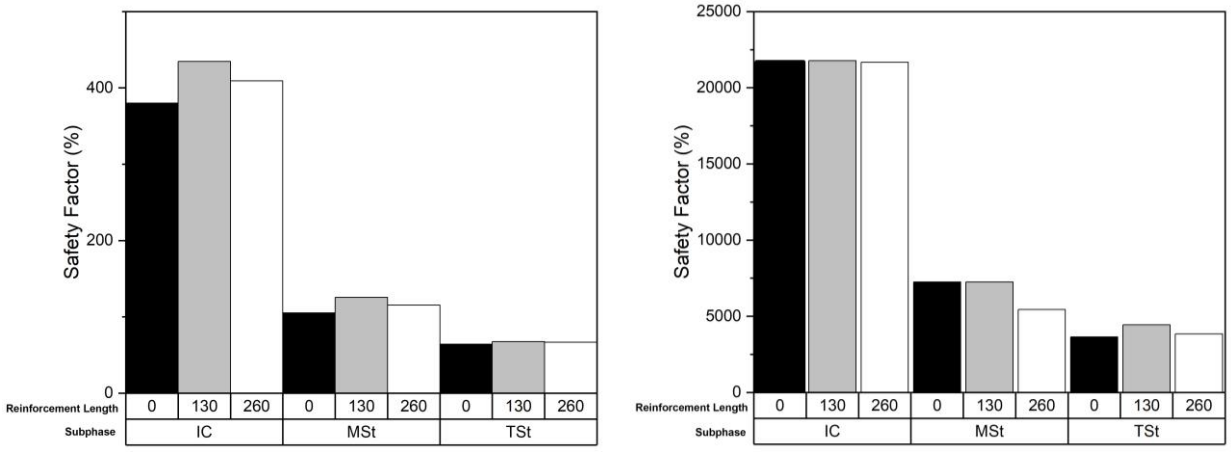

(a) (b)

Fig. 6. Safety Factor of Three SAFO Models with Different Structural Reinforcement in Three Subphases (Initial Contact, Midstance, and Terminal Stance): (a) PP and (b) CF

The deformation result of the simulation was used to calculate the rotational angle and rotational stiffness. The rotational stiffness defines how far the SAFO can bend during walking. The purpose of SAFO is to provide stability to the user so that the user can maintain his posture. So, SAFO should have a low rotational angle or high rotational stiffness to perform its function. The rotational angle and rotational stiffness of SAFO model with different materials and reinforcement lengths are shown in Figure 7.

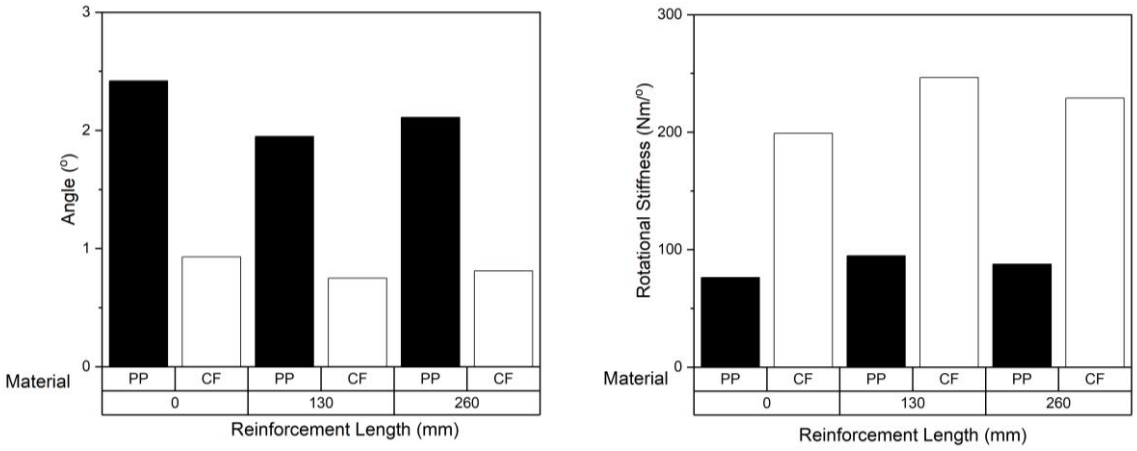

Fig. 7. The Angle and Rotational Stiffness of SAFO Models Based on Their Material and Reinforcement Length

4. DISCUSSION

The Effect of Material Choice

Regarding material choice, CF SAFO models gave lower deformation results in the simulation of cuff loading than PP SAFO. The deformation result was inversely proportional to the stiffness level of each model. Materials with high structural stiffness produce minor deformation when subjected to forces [17]. For example, the cuff loading of PP SAFO variation III (with 260 mm reinforcement) had a rotational stiffness of 87.67 Nm/°. On the other hand, the CF SAFO variation III yielded a rotational stiffness of 228.99 Nm/°. The AFO models that have a better level of stiffness would lead to a better effect on patients in cases of stroke with weakened tibialis anterior and calf muscles [23], [24]. Higher rotational stiffness would provide more stability to the ankle of the users because higher force is needed to bend the SAFO.

Comparing stress results in gait cycle simulation regarding material difference showed that CF SAFO yielded a lower maximum stress value than PP SAFO. For example, PP AFO variation I (without reinforcement) during terminal stance had the maximum von Mises stress of 46.836 MPa. CF AFO variation I during the same phase produced the maximum von Mises stress of 43.959 MPa.

The safety factor obtained after analyzing the maximum stress showed that CF SAFO was far superior to PP SAFO. The CF SAFO model simulation stress in all phases and variations had values lower than the material's ultimate tensile strength. The safety factor of the CF SAFO model in all phases and variations yields results above 100%. This result showed that all CF SAFO variation models were safe for use during the gait cycle. Considering the high safety factor calculation results in CF SAFO, the thickness of the CF SAFO to be manufactured can be reduced due to material and cost efficiency for future possibilities [25].

The Effect of Structural Reinforcement Length

The stress on variation in the reinforcement length showed a decrease in the von Mises stress as the length of applied support increased. This result can be observed from the von Mises stress results in variation III (with 260 mm reinforcement), yielding the lowest stress compared to other model variations under the same gait subphase and material. This result was suitable with the study of Gomes et al. [16], which showed that the stress decreased along with increasing the length of the applied reinforcement.

The decrease in stress distribution obtained during the gait simulation and the increase in the reinforcement length were due to a change in the SAFO geometry. The longer the support used in the model, the more the model's geometry would be in terms of volume. This higher model volume caused the stress to be distributed to more elements. This condition reduced the stress results obtained during gait simulation [24].

The maximum stress in all gait simulations was found in the ankle trimline area. The function of a SAFO that provides ankle stability to the patient requires high rigidity in the ankle trimline area [26]. This condition results in a low flexion tolerance in that area. Under this circumstance, that specific area will experience a higher stress concentration than others, making it vulnerable to cracks [22].

The comparison of deformation during cuff loading simulation showed a decrease in the deformation as the reinforcement length increased. These results indicated that the reinforcement affects the geometry of the designed SAFO model. The deformation obtained showed the level of structural stiffness of each SAFO model variation. For PP, the highest level of stiffness was

obtained in variation II with a value of 94.88 Nm/°. Variation model II also yielded the highest level of stiffness in CF material with a value of 246.52 Nm/°.

The effect of increased stress due to the high moment arm during terminal stance is evident in the stress results of all the PP SAFO variations. All of the safety factors of PP SAFO during terminal stance yield below 100%. This result showed that the increasing stress during terminal stance exceeded the ultimate tensile strength of PP. In this condition, all variations of the PP SAFO will be prone to fail during terminal stance, causing cracks to appear in ankle trimlines where the maximum stresses accumulate [22].

Despite this, when SAFO is applied, the terminal stance will be eliminated due to its high rigidity. Therefore, although the PP SAFO simulation during terminal stance in all variations experienced failure due to cracks, PP SAFO is still safe for patient use because the terminal stance has been eliminated in the first place.

5. CONCLUSIONS

In general, the toughness of SAFO to the forces that occur during the stance phase of the gait cycle would increase as the length of applied reinforcement increases. Comparing the material difference during the simulations under the same variations and phases, it can be concluded that CF SAFO provides better toughness than PP SAFO. A comparison of simulation results in terms of the reinforcement length showed that the structural stiffness level in the SAFO model would increase as the length of applied reinforcement increases. Furthermore, under the same variety of support, CF SAFO gives a better stiffness level than PP SAFO.

CF SAFO variation II gives the best parameter combination. Based on safety factor calculation, the model has the highest result at each phase of the gait cycle that has been simulated. In terms of the level of stiffness to provide more ankle stability, the CF SAFO variation II also gives the best results with a ratio of 246.52 Nm/°. Dynamic loading should improve the simulation results approach to the initial gait cycle. Fatigue analysis can also be carried out to examine the behavior of the SAFO model on repeated use.

ACKNOWLEDGEMENTS

We would like to thank Universitas Airlangga, who funds this study under the scheme of Young Lecturer Research 2019.

CONFLICT OF INTERESTS

The authors declare that there is no conflict of interests.

REFERENCES

[1] M. Alam, I.A. Choudhury, A.B. Mamat, Mechanism and design analysis of articulated ankle foot orthoses for drop-foot, Sci. World J. 2014 (2014), 867869. https://doi.org/10.1155/2014/867869.

[2] M. Paoloni, M. Mangone, P. Scettri, et al. Segmental muscle vibration improves walking in chronic stroke patients with foot drop: a randomized controlled trial, Neurorehabil. Neural Repair. 24 (2009), 254-262. https://doi.org/10.1177/1545968309349940.

[3] A. Daryabor, M. Arazpour, G. Aminian, Effect of different designs of ankle-foot orthoses on gait in patients with stroke: A systematic review, Gait Posture. 62 (2018), 268-279. https://doi.org/10.1016/j.gaitpost.2018.03.026.

[4] M. Hamedi, P. Salimi, A. Aliabadi, et al. Toward intelligent ankle foot orthosis for foot-drop, a review of technologies and possibilities, in: 2015 2nd International Conference on Biomedical Engineering (ICoBE), IEEE, Penang, 2015: pp. 1-6. https://doi.org/10.1109/ICoBE.2015.7235875.

[5] A. Sturma, O. Schuhfried, T. Hasenoehrl, et al. The long-term effects of an implantable drop foot stimulator on gait in hemiparetic patients, PLoS ONE. 14 (2019), e0214991. https://doi.org/10.1371/journal.pone.0214991.

[6] C. Stewart, A.P. Shortland, The biomechanics of pathological gait - from muscle to movement, Acta Bioeng. Biomech. 12 (2010), 3-12.

[7] M. Hamedi, P. Salimi, A. Aliabadi, M. Vismeh, Toward intelligent ankle foot orthosis for foot-drop, a review of technologies and possibilities, in: 2015 2nd International Conference on Biomedical Engineering (ICoBE), IEEE, Penang, 2015: pp. 1–6. https://doi.org/10.1109/ICoBE.2015.7235875.

[8] A.E. Chisholm, S.D. Perry, Ankle-foot orthotic management in neuromuscular disorders: recommendations for future research, Disabil. Rehabil.: Assist. Technol. 7 (2012), 437-449. https://doi.org/10.3109/17483107.2012.680940.

[9] A. Abdelkader, Immediate effect of solid ankle foot orthosis versus ground reaction ankle foot orthosis on balance in children with spastic diplegia, Biosci. Res. 15(2018), 1893-2898.

[10] H.K. Surmen, N.E. Akalan, Y.Z. Arslan, Design, manufacture, and selection of ankle-foot-orthoses, in: M. Khosrow-Pour, ed., Advanced methodologies and technologies in artificial intelligence, computer simulation, and human-computer interaction, IGI Global, Hershey, PA, 2019, 298-313. https://doi.org/10.4018/978-1-5225-2255-3.ch027.

[11] A. Ielapi, N. Lammens, W. Van Paepegem, et al. A validated computational framework to evaluate the stiffness of 3D printed ankle foot orthoses, Computer Methods Biomech. Biomed. Eng. 22 (2019) 880-887. https://doi.org/10.1080/10255842.2019.1601712.

[12] S. Syngellakis, M.A. Arnold, Modelling considerations in finite element analyses of ankle foot orthoses, WIT Trans. Ecol. Environ. 160 (2012), 183-194.

[13] A.P. Putra, A. Rahmatillah, N.K. Rodhiyah, et al. Computational analysis of ankle-foot orthosis for foot drop case during stance phase in gait cycle, J. Eng. Sci. Technol. 17 (2022), 985-996.

[14] A.P. Putra, A. Rahmatillah, Pujiyanto, et al. Computational study of ventral ankle-foot orthoses during stance phase for post-surgery spinal tuberculosis rehabilitation, in: Triwiyanto, H.A. Nugroho, A. Rizal, W. Caesarendra (Eds.), Proceedings of the 1st International Conference on Electronics, Biomedical Engineering, and Health Informatics, Springer Singapore, Singapore, 2021: pp. 447-455. https://doi.org/10.1007/978-981-33-6926-9_38.

[15] R.K. Chen, L. Chen, B.L. Tai, et al. Additive manufacturing of personalized ankle-foot orthosis, in: Proceedings of NAMRI/SME, (2014).

[16] G. Gomes, I. Lourenco, J. Oliveira, et al. Structural reinforcements on AFO's: A study using computer-aided design and finite element method, in: 2017 IEEE 5th Portuguese Meeting on Bioengineering (ENBENG), IEEE, Coimbra, Portugal, 2017: pp. 1-4. https://doi.org/10.1109/ENBENG.2017.7889432.

[17] M.H. Bagherinejad, R. Kamgar, Improvement of the results of finite element method in plate analysis using mesh sizing modifying function, Int. J. Integr. Eng. 12 (2020), 31-43.

[18] H. Patil, P.V. Jeyakarthikeyan, Mesh convergence study and estimation of discretization error of hub in clutch disc with integration of ANSYS, IOP Conf. Ser.: Mater. Sci. Eng. 402 (2018), 012065. https://doi.org/10.1088/1757-899x/402/1/012065.

[19] H. Basri, A. Syahrom, T.S. Ramadhoni, et al. The analysis of the dimple arrangement of the artificial hip joint to the performance of lubrication, IOP Conf. Ser.: Mater. Sci. Eng. 620 (2019), 012116. https://doi.org/10.1088/1757-899x/620/1/012116.

[20] H. Zamanian, Toward creating normal ankle joint behavior for drop foot patients using an ankle foot orthosis (AFO) with superplastic NiTi springs, Ph.D. Thesis, College of Graduate Studies, The University of Toledo, Toledo, Spain, (2017).

[21] J. Pratama, M. Mahardika, Finite element analysis to determine the stress distribution, displacement and safety factor on a microplate for the fractured jaw case, AIP Conf. Proc. 1941 (2018), 020022, https://doi.org/10.1063/1.5028080.

[22] M. Volpini, D. Alves, A. Horta, et al. Orthosis and finite elements: a study for development of new designs through additive manufacturing, Int. J. Biomed. Biol. Eng. 12 (2018), 262-266. https://doi.org/10.5281/zenodo.1317112.

[23] E. Kerr, K. Moyes, G. Arnold, et al. Permanent deformation of posterior leaf-spring ankle-foot orthoses: a comparison of different materials, J. Prosthet. Orthot. 23 (2011), 144-148. https://doi.org/10.1097/jpo.0b013e3182272941.

[24] D.J.J. Bregman, V. De Groot, P. Van Diggele, et al. Polypropylene ankle foot orthoses to overcome drop-foot gait in central neurological patients, Prosthet. Orthot. Int. 34 (2010), 293-304. https://doi.org/10.3109/03093646.2010.495969.

[25] D. Totah, I. Kovalenko, M. Saez, et al. Manufacturing choices for ankle-foot orthoses: a multi-objective optimization, Procedia CIRP. 65 (2017), 145-150. https://doi.org/10.1016/j.procir.2017.04.014.

[26] S. Syngellakis, M.A. Arnold, H. Rassoulian, Assessment of the non-linear behaviour of plastic ankle foot orthoses by the finite element method, Proc. Inst. Mech. Eng. Part H: J. Eng. Med. 214 (2000), 527-539. https://doi.org/10.1243/0954411001535561.